

- 5 (1973). The list is not exhaustive. Carbon relaxation has also been studied in complex natural products that contain saturated heterocyclic rings, e.g., stachyose, A. Allerhand and D. Dodderell, *J. Am. Chem. Soc.*, **93**, 2777 (1971).
- (3) For a review, see J. B. Lambert and S. I. Featherman, *Chem. Rev.*, **75**, 611 (1975).
- (4) Nomenclature has been discussed in the previous paper.⁵
- (5) J. B. Lambert, D. A. Netzel, H.-n. Sun, and K. K. Lilianstrom, *J. Am. Chem. Soc.*, preceding paper in this issue.
- (6) For reviews, see E. Breitmaier, K.-H. Spohn, and S. Berger, *Angew. Chem., Int. Ed. Engl.*, **14**, 144 (1975); J. R. Lyster, Jr., and G. C. Levy, *Top. Carbon-13 NMR Spectrosc.*, **1**, 79 (1974).
- (7) This stack of real spectra was obtained with the assistance of Dr. W. W. Conover of the University of Chicago. All reported data unless otherwise noted were obtained at Northwestern University from magnitude spectra.
- A comparison of T_1 obtained from the real and the magnitude spectra showed no differences.
- (8) D. A. Netzel, Ph.D. Dissertation, Northwestern University, 1975.
- (9) We thank Dr. W. W. Conover for the program DNT1CAL and Dr. R. J. Bastasz for the program DNB05 and their adaptation to the Nova 840.
- (10) N. Bloembergen, E. M. Purcell, and R. V. Pound, *Phys. Rev.*, **73**, 679 (1948); also see, J. R. Lyster, Jr., Ph.D. Dissertation, University of Utah, 1971.
- (11) D. E. Woessner, B. S. Snowden, Jr., and E. T. Strom, *Mol. Phys.*, **14**, 265 (1968); D. E. Woessner, *J. Chem. Phys.*, **37**, 647 (1962).
- (12) J. B. Lambert, R. G. Keske, R. E. Carhart, and A. P. Jovanovich, *J. Am. Chem. Soc.*, **89**, 3761 (1967).
- (13) S. Berger, F. R. Kreissl, and J. D. Roberts, *J. Am. Chem. Soc.*, **96**, 4348 (1974).
- (14) G. C. Levy, *J. Chem. Soc., Chem. Commun.*, 47 (1972).
- (15) See Table II in ref 3.

Studies on the ^1H and ^{13}C Contact Shifts for σ -Bonded Molecules.¹ Stereospecific Electron Spin Transmission in Cyclic and Bicyclic Amines

Isao Morishima,* Kenichi Yoshikawa, and Koji Okada

Contribution from the Department of Hydrocarbon Chemistry, Faculty of Engineering, Kyoto University, Kyoto, Japan. Received September 2, 1975

Abstract: ^1H and ^{13}C NMR contact shifts induced by nickel acetylacetonate ($\text{Ni}(\text{AA})_2$) have been observed for various cyclic and bicyclic amines. These contact shifts are well reproduced by INDO molecular orbital calculations of spin densities on the proton $1s$ and carbon $2s$ atomic orbitals for the corresponding hydrocarbon σ radicals. It is shown that the proton contact shifts follow the stereospecificity established for nuclear spin-spin coupling constants. The importance of the *through-space* spin transfer in the rigid σ -bonded skeleton is also proposed to account for the nonalternating feature of ^{13}C contact shifts for planar zigzag arrangement of the σ skeleton. This mechanism is also discussed in relation to the long-range H-H coupling constant across four σ bonds.

We have currently been interested in the stereospecificity of the mode of electron spin distribution through the σ skeleton in view of elucidation of the σ -electronic structures. We have previously reported² the proton and carbon-13 contact shifts for N-heterocyclic molecules complexed with paramagnetic nickel acetylacetonate ($\text{Ni}(\text{AA})_2$).^{3,4} In these studies it has been demonstrated that the relative contact shifts of various protons and carbons definitely depend on the conformation or configuration of the intervening σ -bonds connecting these and the nitrogen atoms. A linear correlation between the $\text{Ni}(\text{AA})_2$ -induced NMR contact shift and the ESR hyperfine coupling constant (hfsc) in an organic free radical with the corresponding isoelectronic structure has recently been demonstrated.^{2,5,6} It has also been shown that NMR contact shifts are quite useful to probe the mechanism of intramolecular electron spin transmission because it is quite sensitive to a small quantity and a sign of the induced spin density.²

The correlation between hyperfine coupling constant (hfsc) of a σ -type radical and the NMR nuclear spin-spin coupling constant (J) for protons has been pointed out theoretically⁷⁻⁹ and experimentally.⁸ The correlation between the contact shifts and the nuclear spin coupling constants (J) has also been studied.^{10,11} The studies on the stereospecific electron spin transmission through the σ skeleton seem to serve as an aid in understanding the electronic structure of σ -bonded molecules. For this purpose, we have extended here our NMR contact shift studies to the various cyclic and bicyclic amines. Our concern in this study is to find the conformational or configurational dependence of electron spin distribution and to elucidate the mechanism of intramolecular electron spin transmission in relation to hfsc's and nuclear spin-spin coupling constants associated with the corresponding σ skeleton.

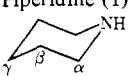
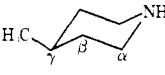
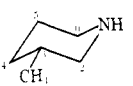
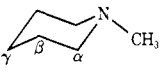
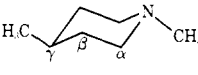
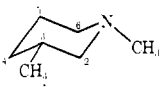
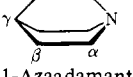
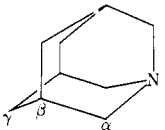
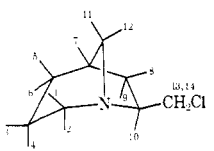
Experimental Section

Materials. Piperidine (1), 4-methylpiperidine (2), 3-methylpiperidine (3), *N*-methylpiperidine (4), and quinuclidine (7) were obtained from commercial sources. 1,4-Dimethylpiperidine (5) and 1,3-dimethylpiperidine (6) were prepared by *N*-methylation of 2 and 3, respectively.¹² 1-Azaadamantane (8) was provided by Dr. W. N. Speckamp. 3,3,4-Trimethyl-2-chloro-1-azabicyclo[2.2.1]heptane (9) was provided by Professor P. G. Gassman. 7-Chloromethyl-1-azabicyclo[3.2.1]octane (10) was a gift from Dr. C. F. Hammer. $\text{Ni}(\text{AA})_2$ was dried in vacuo over 30 h at 60 °C before use.

Proton NMR Measurements. All the proton spectra were obtained at 220 MHz using a Varian HR-220 spectrometer in our department. Me_4Si was used as an internal standard. The samples were made in 10% v/v CDCl_3 solutions for piperidine derivatives (1-6), in ca. 0.1 M CDCl_3 solutions for 7 and 8, and in 0.5 M CDCl_3 solution for 10. Assignment of proton signals was made by referencing the spectral patterns, the europium dipivalomethane ($\text{Eu}(\text{dpm})_3$), and cobalt acetylacetonate ($\text{Co}(\text{AA})_2$) induced pseudocontact shifts. The variation of the spectral patterns were also referred. Signal assignments of 10 remain somewhat speculative.

^{13}C NMR Measurements. Completely proton decoupled ^{13}C NMR spectra were obtained at 25.15 MHz on a JEOL-JNM-PFT-100 system. After the ~ 100 -30000 accumulations of the free induction decays induced by the 45° pulses with the interval of 2-4 s, the Fourier-transformed spectra were recorded. The ^{13}C spectra were obtained from a CDCl_3 solution of 9 in 0.5 M, 10 in 3 M, and 3 in 50% v/v. The spectra were taken at room temperature (24°) in the presence of varying amounts of $\text{Ni}(\text{AA})_2$ as in the case of ^1H NMR measurements. The ^{13}C chemical shifts were measured with respect to internal Me_4Si or CDCl_3 (77.1 ppm from Me_4Si). The assignments of ^{13}C NMR spectra were made by referring the shifts of related compounds^{2d,f,13} and by the use of the stereospecific ^{13}C contact shift induced by $\text{Ni}(\text{AA})_2$.^{2b-e} The half-decoupled technique was used to help the signal assignment of the ^{13}C NMR spectra.

Table I. Relative ¹H Contact Shifts for Various N-Containing Molecules Complexed with Ni(AA)₂^a

Ligand molecules	Position	Chemical shift ^b ¹ H (δ)	Rel contact shift	
Piperidine (1) 	α	2.80	-1.00 ^e	
	β	1.54	-0.35	
	γ		-0.15	
4-Methylpiperidine (2) 	α {ax	2.58	-1.00 ^e	
	α {eq	3.04	-0.77	
	β {ax	1.08	+0.11	
	β {eq	1.62	-0.67	
	γ ax	1.45	-0.09	
3-Methylpiperidine (3) 	α {2-ax	2.20	-1.00 ^e	
	α {6-ax	2.52	-1.00	
	α {2,6-eq	2.99	-0.64	
	β {3,5-ax	1.50	+0.02	
	β {5-eq	1.63	^c	
	γ {ax	1.01	-0.05	
	γ {eq	1.77	-0.14	
<i>N</i> -Methylpiperidine (4) 	α	2.34	-1.00 ^f	
	β	1.60	+0.04	
	γ	1.42	-0.04	
1,4-Dimethylpiperidine (5) 	α {ax	1.91	-1.00 ^f	
	α {eq	2.72	-0.38	
	β {ax	1.3	+0.09	
	β {eq	1.63	-0.03	
	γ ax	1.36	+0.04	
1,3-Dimethylpiperidine (6) 	α {2-ax	1.52	-1.00 ^f	
	α {6-ax	1.80	-1.00	
	α {2,6-eq	2.78	-0.36	
	β {3,5-ax	1.65	+0.08	
	β {5-eq		-0.07	
	γ {eq	0.83	+0.08	
	γ {ax		+0.04	
Quinuclidine (7) 	α	2.87	-1.00 ^g	
	β	1.55	-0.10	
	γ	1.76	+0.10	
1-Azaadamantane (8) 	α	3.17	-1.00 ^h	
	β	1.71	-0.77	
	γ {ax	2.00	-0.02	
	γ {eq	1.93	-0.30	
1-Aza-7-chloromethylbicyclo[3.2.1]octane (10) 	1	2.86	-0.70	
	2	2.86	-0.34	
	3	1.36	-0.24	
	4	1.68	+0.11	
	5	1.6	-0.12	
	6	1.6	-0.11	
	7	2.27	-0.31	
	8	1.6	-0.17	
	9	1.95	+0.04	
	10	3.49	-0.11	
	11	2.73	-0.01	
	12	2.73	-1.00 ^f	
	CH ₂ Cl	13	3.3 ^d	-0.11
		14	3.3 ^d	-0.01

^a Measured in CDCl₃ solution. ^b In parts per million from Me₄Si. ^c A relatively large downfield shift. Because of signal broadening, precise value could not be obtained. ^d Two methylene protons were observed separately. As the relative Ni(AA)₂-induced shifts are markedly different from each other, the rotation around the C(7)-CH₂Cl bond is considered to be forbidden due to the steric hindrance. ^e The actual shift is ca. 0.3 ppm per 0.05 mol of Ni(AA)₂ in the 10% v/v solution. ^f The actual shift is ca. 0.5 ppm per 0.05 mol of Ni(AA)₂ in the 10% v/v solution. ^g The actual shift is 0.4 ppm per 0.01 mol of Ni(AA)₂ in the 0.1 M solution. ^h The actual shift is 1.2 ppm per 0.01 mol of Ni(AA)₂ in the 0.1 M solution. ⁱ The actual shift is 1.0 ppm per 0.05 mol of Ni(AA)₂ in the 0.5 M solution.

Results and Discussion

Stereospecific Proton Contact Shifts and Electron Spin Distribution. In piperidine (1) and *N*-methylpiperidine (4), the ring inversion rate is so rapid at room temperature that only the time-averaged signals of axial and equatorial protons are observed for α, β, and γ protons. Introduction of a methyl group in the piperidine ring slows down this inversion rate and the separated signals of axial and equatorial protons of α and β methylene groups were obtained. Spectral assignments for symmetrical molecules (1, 2, 4, 5, 7, 8) follow directly from the relative intensities and splitting patterns of well-separated signals. For the other molecules (3, 6, 10) proton spectra are more complicated even at 220 MHz, but with the aid of Co(AA)₂ or Eu(dpm)₃-induced shifts, we are able to definitely assign each signal. The resonance positions are summarized in Table I. The perturbation of the NMR spectra of 1-azaadamantane (8) and 1-aza-7-chloromethylbicyclo[3.2.1]octane (10) induced by Ni(AA)₂ are shown in Figures 1 and 2, respectively. In Figure 3 is exemplified a plot of paramagnetic shift vs. the concentration of Ni(AA)₂ for 10. Each proton resonance is shifted from its normal diamagnetic value by an amount which is proportional to the concentration of added Ni(AA)₂. This linear relation implies that the exchange of ligand between complexes and uncomplexed sites is time averaged. Thus the proton resonances of the ligand shift toward the resonance position of the complex as Ni(AA)₂ is added to the diamagnetic solution and the relative values of these shifts are significant in the present study. The relative values for various protons in a ligand molecule were obtained from the slope of the linear plot of the paramagnetic shift vs. the concentration of Ni(AA)₂, with the value for an α proton normalized to 1.00. The relative proton contact shifts for various ligand molecules are also summarized in Table I. The (+) and (-) signs correspond to the negative and the positive spin densities induced on the ligand proton, respectively. In this table, the relative paramagnetic shifts of β and γ protons in 1, where no separated signals of the axial and the equatorial protons are observed, are nearly the average of the shifts of axial and equatorial protons in 2 or 3. This is also the case for *N*-methylpiperidine (4), as an average of 5 or 6.

It has been well established that the isotropic proton paramagnetic shift in the Ni(AA)₂ system is resulting most dominantly from the Fermi contact shift which is related to the electron spin density distributed on the proton. For piperidine (1), all the ring protons experiences downfield contact shifts, while in *N*-methylpiperidine (4) β protons exhibit upfield shifts. This different feature of the contact shift is more apparent in 2 and 5. For 2, the β-equatorial proton shows large downfield contact shift, while the β-axial one exhibits quite a small upfield contact shift. For 5, on the contrary, the β-equatorial proton experiences a downfield shift and the axial one shows a large upfield shift.

It has been shown^{2a,c,d} that in *N*-H piperidines the lone-pair electrons occupy an equatorial position at least in the complex with Ni(AA)₂, while in *N*-methylpiperidine the lone-pair axial conformer is favorable. Therefore, the different feature of the β-proton contact shifts between *N*-H and *N*-methylpiperidine is attributed to the effect of different lone-pair orientation. Accordingly, the large downfield shift for the β-equatorial proton in *N*-H piperidines (1, 2, 3) and 1-azaadamantane may result from the positive spin density transferred through a "zigzag" path of the σ skeleton. The downfield and upfield contact shifts in 1 and 4, in which the β-proton signal is observed as an average of the resonances of axial and equatorial protons, also reflect the specific shifts for β protons due to the different lone pair orientation.

Thus, conformational dependence on the ¹H contact shift due to the different lone pair orientation is shown below. In a

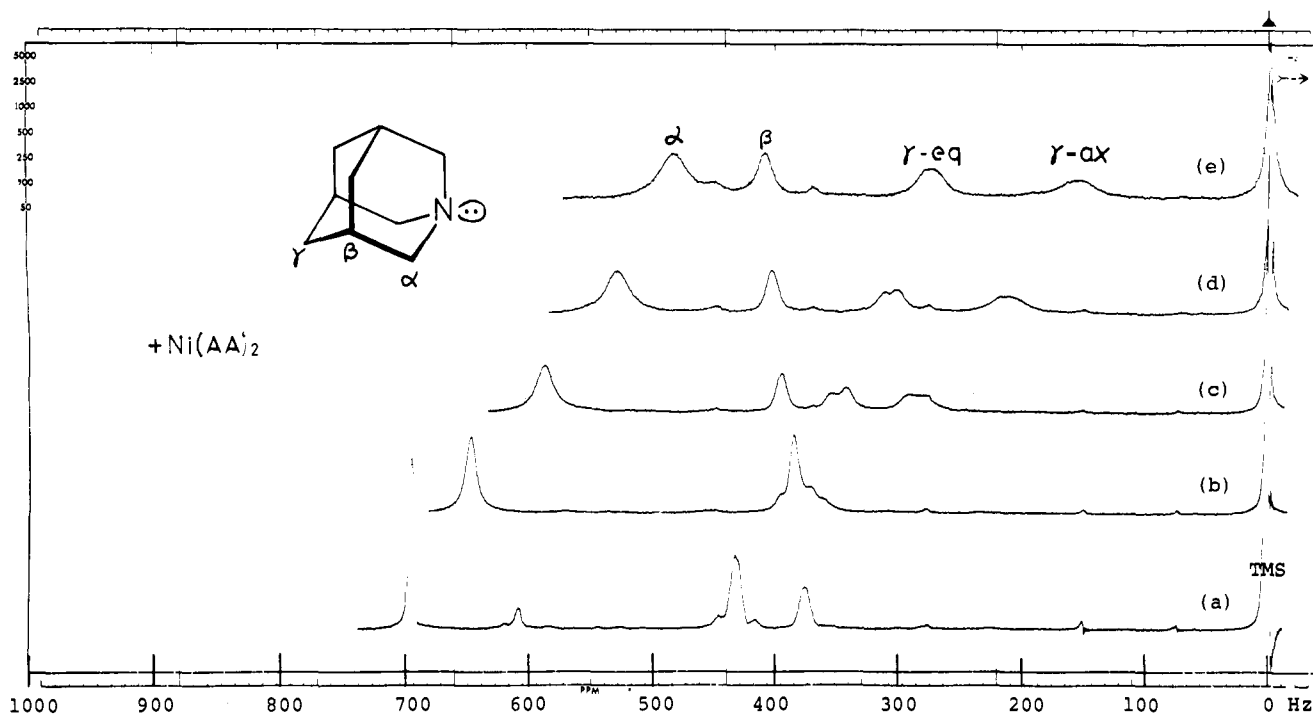


Figure 1. The 220-MHz ^1H NMR spectra of **8**: (a) in CDCl_3 and (b–e) in CDCl_3 containing varying amounts of $\text{Ni}(\text{AA})_2$.

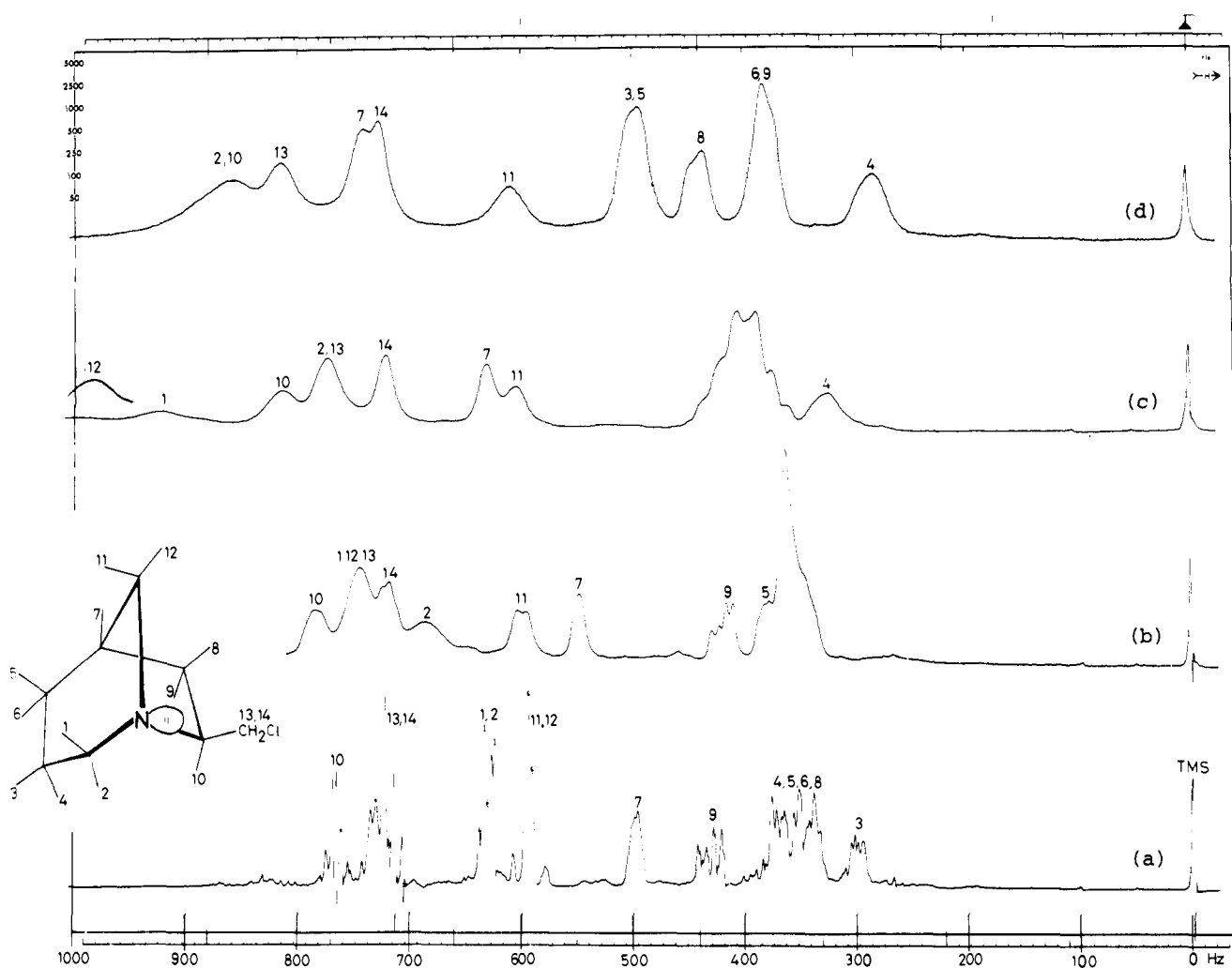


Figure 2. The 220-MHz ^1H NMR spectra of **10**: (a) in CDCl_3 and (b–d) in CDCl_3 containing varying amounts of $\text{Ni}(\text{AA})_2$.

lone pair equatorial conformer (**1**, **2**, **3**, **8**), the downfield contact shifts for the equatorial protons attenuate slowly

through the σ skeleton, but rapidly for the axial protons. While in a lone pair axial conformer, the contact shifts attenuate

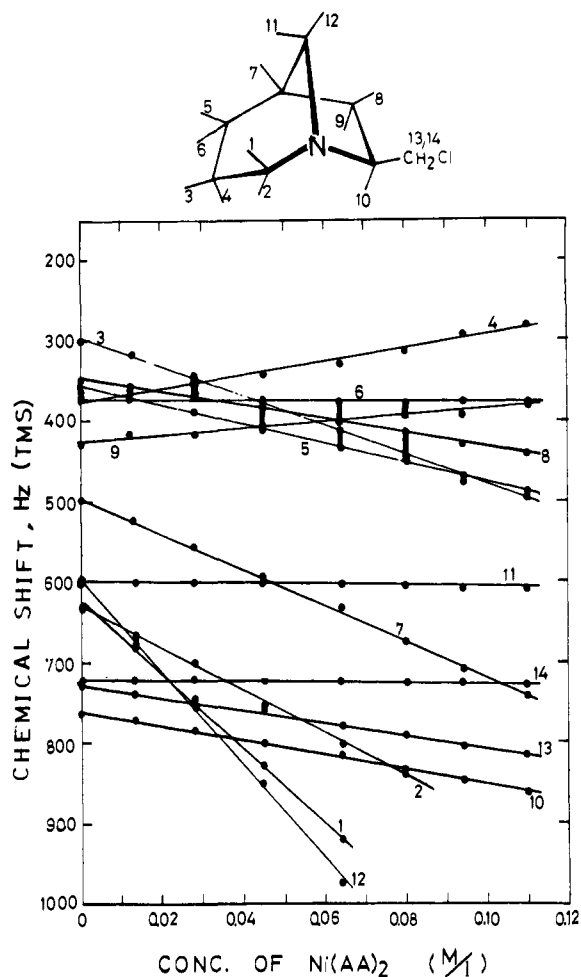
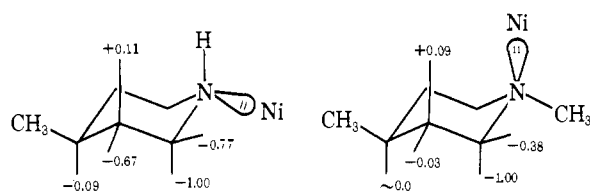
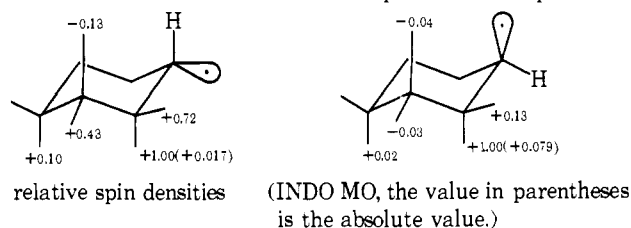


Figure 3. Plots of isotropic paramagnetic ^1H shifts vs. concentration of $\text{Ni}(\text{AA})_2$ for **10**.



rapidly for both the equatorial and the axial protons, and this attenuation is more prominent for the equatorial protons than for the axial ones. In this conformer the substantial upfield contact shift for the β protons is quite characteristic. In both cases the proton separated by "zigzag" σ bonds from the nitrogen-metal bond exhibits greater contact shift than that separated by "folded" bonds.

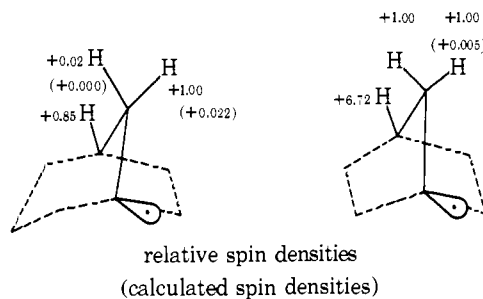
These stereospecific features of ^1H contact shifts are plausibly reproduced by the molecular orbital calculations of electron spin densities distributed on the proton for the corresponding hydrocarbon σ radicals. We have carried out INDO-UHF MO calculations for the two conformers of the cyclohexyl radical in which the orientation of the radical lobe are in the axial and equatorial positions. The results are shown below. Correspondence between the relative values of ^1H contact shifts and those of calculated spin densities is plausible.



From the above results, one can see the typical behavior of the electron spin distribution on the protons through the σ skeleton and the mechanism of electron spin transmission. Electron spin may reach the ligand protons by two different mechanisms, spin delocalization (SD) and spin polarization (SP), as schematically represented below. (1) Positive spin

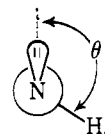


density (\uparrow) reaches the proton by the direct electron delocalization, which is proportional to the hydrogen and carbon s orbital contribution to the molecular orbital containing an unpaired electron. (2) Negative spin density (\downarrow) is induced by spin polarization mechanism. The delocalization mechanism gives rise to the downfield contact shifts of all the protons, but the spin polarization mechanism leads to alternation and attenuation of the shifts along the σ -bonds. In the actual cases, these two mechanisms may be simultaneously operating. The upfield or downfield contact shift of γ protons in piperidines depends on whether the SP or SD mechanism is dominant. It should be noted that in **9** the α -proton contact shifts are quite different in magnitude to each other. For example, the contact shift for the α proton attached to the bridgehead carbon is about 50 times larger than that for H_{11} . This is also reproduced by INDO calculations of the spin densities for the corresponding hydrocarbon σ radical. For a model of this radical we examined the propyl radical^{14,15} with planar and nonplanar geometries, which constitutes a part of 1-bicyclo[3.2.1]heptyl



radical and 1-bicyclo[2.2.1]hexyl radical, respectively. The calculated spin densities for the nonplanar model agree well with the observed results. It is therefore recognized that proton contact shifts are remarkably sensitive to the molecular configuration.

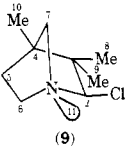
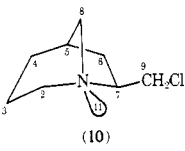
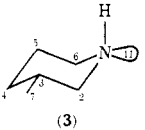
It has already been shown that in piperidine the α -axial proton in the lone-pair axial conformer senses positive spin density three times as large as the α -equatorial proton. Accordingly, the large shift of H_{12} in **9** is due to the planar trans (180°) conformation, and the abnormally small shift for H_{11}



is due to the conformation in which the angle (θ) between the lone pair orientation and the C-H bond is close to 90° . Consequently, one can find the trend of ^1H NMR contact shifts in the H-C-N skeleton correspond well to the " $\cos^2 \theta$ rule" well established for the vicinal H-H coupling constant.¹⁶

In order to gain further insight into such a relation, we performed a calculation of electron spin densities (ρ_{UHF}) on the protons in the ethyl σ radical, which corresponds to the H-C-N σ -fragment complexed with $\text{Ni}(\text{AA})_2$. In Figure 4 is shown the angular dependence of the induced electron spin density (ρ_{UHF}) on the C(2) proton. The geometry of ethyl

Table II. ^{13}C Contact Shifts for Azacyclic Molecules

Molecules	Position	^{13}C chem shift, ^a ppm	^{13}C contact shift ^b (rel value)
 (9)	2	92.8	+0.48
	3	49.5 ^c	- ^d
	4	45.0 ^c	- ^d
	5	30.5	-0.66
	6	51.3	+1.00 ^e
	7	58.5	+0.37
	8	21.0	-0.13
	9	20.2	+0.05
	10	10.1	-0.14
	 (10)	2	56.3 ^c
3		20.1	-0.65
4		30.7	+0.08
5		36.4	-0.84
6		36.4	-0.98
7		64.8	+0.25
8		59.1 ^c	+0.78
9 (CH ₂ Cl)		48.5	-0.55
 (3)		2	55.0
	3	32.7	-1.2
	4	34.3	+0.11
	5	27.3	-1.2
	6	47.3	+0.94
	7	20.2	-0.23

^a Chemical shifts are given in parts per million from Me₄Si. ^b The (+) and (-) signs denote the upfield and downfield contact shifts, respectively. The relative shifts were obtained from the slope of the linear plot of the observed contact shift vs. the concentration of added Ni(AA)₂. ^c The signal assignment is somewhat uncertain. ^d The signal broadening was too great to get the precise magnitude of the relative downfield contact shift. ^e The actual shift is 7 ppm per 0.02 mol of Ni(AA)₂ in the 0.5 M CDCl₃ solution. ^f The actual shift is 1.0 ppm per 0.08 mol of Ni(AA)₂ in the 3 M CDCl₃ solution. ^g The actual shift is 5 ppm per 0.05 mol of Ni(AA)₂ in the 50% v/v CDCl₃ solution.

radical was taken as C-C = 1.54 Å, C-H = 1.09 Å, and any bond angle = 109° 28'. Inspection of this figure shows that the value of ρ_{UHF} follows the angular dependence of the "cos² θ rule". In this figure, ρ_{UHF} is separated into the two contributions of spin transmission mechanism, SP and SD, based on the method proposed by Nakatsuji et al.¹⁷ It is worth noting that the angular dependence of ρ_{SD} as well as that of ρ_{SP} resembles to the "cos² θ rule". This is the reason why the relative values of isotropic hyperfine coupling constants agree well with those of nuclear spin coupling constants, which is determined by the spin polarization mechanism.

^{13}C Contact Shift and Mechanism of Intramolecular Spin Transmission through the σ Skeleton. In the previous section, we studied stereospecific ^1H contact shifts for six-membered amines. We concluded that these contact shifts are associated with spin densities distributed on the proton and are characteristic of an axially or equatorially oriented nitrogen lone pair and configuration or conformation of the carbon skeleton. In order to gain further insight into the stereospecific mode of electron spin distribution and the mechanism of intramolecular spin transmission through the σ skeleton, we have studied here ^{13}C contact shift for 1-azanorbornene derivative and 1-azabicyclo[3.2.1]octane derivatives.

We have already reported in the previous papers^{2c,d} the Ni(AA)₂-induced ^{13}C contact shifts for piperidine, 4-methylpiperidine, *N*-methylpiperidine, 1,4-dimethylpiperidine, quinclidine, and 1-azaadamantane. An alternation in sign and attenuation in magnitude of the ^{13}C contact shifts have been obtained in these compounds. For example, in 1-azaadamantane with a rigid chain conformation, Ni(AA)₂-induced spin densities on the carbon atoms were alternating in sign along the bond as is always the case for piperidine derivatives and

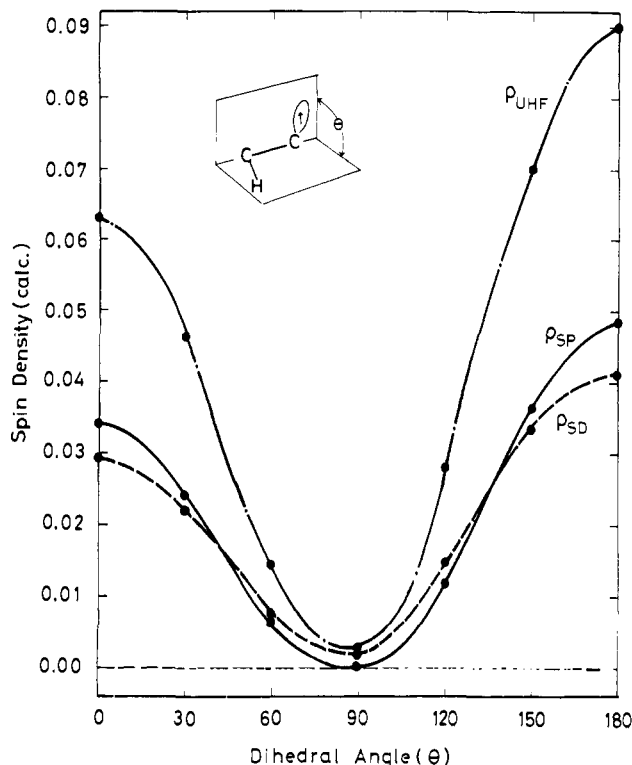
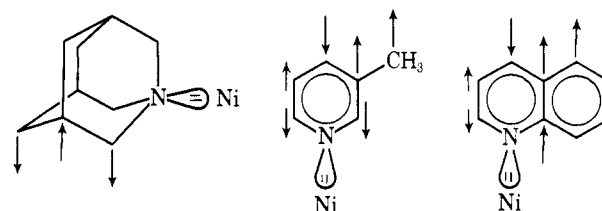


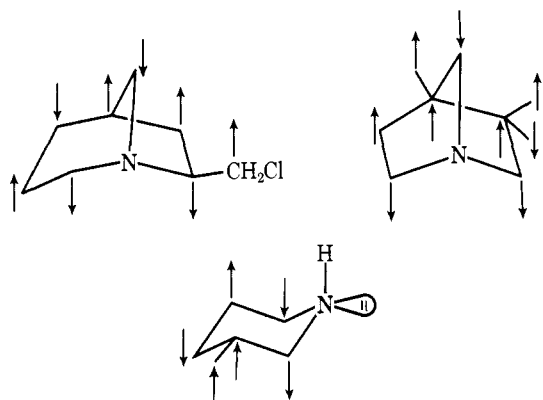
Figure 4. Angular dependence of ρ_{UHF} , ρ_{SP} , ρ_{SD} induced on C(2)-H proton (INDO UHF MO).

pyridine.^{2c,d} Such an alternation of ^{13}C contact shifts has been attributed to the preferential contribution of the spin polarization mechanism. In contrast to this, nonalternation of the sign of the spin density was encountered for the γ carbons, such as the methyl carbon of β -picoline¹⁸ and the C(5)-carbon of quinoline.^{2c} The positive spin density on these γ -carbon atoms



could not be expected by inspection of the normal mode of spin transmission along the N-C α -C β -C γ skeleton with alternating signs. In order to further examine such a stereospecific feature of electron spin transmission through the σ -skeleton, in Table II are presented the ^{13}C contact shifts for 3,3,4-trimethyl-2-chloro-1-azabicyclo[2.2.1]heptane (9), 7-chloro-1-azabicyclo[3.2.1]octane (10), and 3-methylpiperidine (3), which involve N-C α -C β -C γ skeletons with different figures of arrangement.

In these compounds, the contact shifts for various γ -carbons are quite different from each other. The γ -carbons C(4) in 10 and C(9) in 9 experience upfield shifts (negative spin densities). On the other hand, the downfield shift for the γ -carbon was encountered for C(8) and C(10) in 9, which are lying on the semiplanar or planar zigzag arrangement of the N-C α -C β -C γ skeleton.¹⁹ This nonalternating nature of the Ni(AA)₂-induced spin densities is quite similar to the case of β -picoline¹⁸ and quinoline.^{2c} It follows, therefore, that when the N-C α -C β -C γ arrangement is a planar or semiplanar zigzag, then the γ -carbon senses the positive spin density, while negative spin is induced for the nonplanar arrangement (C γ of piperidine, *N*-methylpiperidine, and 1-azaadamantane, C(4) of 10, and C(9) of 9), as is depicted below. Such a trend is also the case



for 3-methylpiperidine (3), in which the lone-pair electrons preferentially occupy the equatorial position. The C(4) carbon in the nonplanar arrangement feels the upfield contact shift, whereas the C(7)-methyl carbon in the planar zigzag conformation senses the downfield shift. The specific mode of electron spin distribution (nonalternation) in the planar zigzag skeleton may allow us to expect a "through-space" spin transmission which could produce positive spin density on the γ carbon due to the direct nitrogen- C_β interaction. The study on such a stereospecific mode of electron spin transmission is expected to shed light on the neighboring σ -bond participation in the σ -electronic system.



In order to gain further insight into this stereospecific spin distribution, we studied INDO-UHF MO calculations of electron spin densities distributed on the carbon atoms for a n -butyl σ radical as a model of a $N-C_\alpha-C_\beta-C_\gamma$ fragment complexed with $Ni(AA)_2$. The experimental trend of alternating and nonalternating spin densities was plausibly reproduced by this model calculation for nonplanar and planar n -butyl σ radicals, respectively (see Table III). It is particularly to be noted that on the C(4) carbon, negative spin is induced in the nonplanar arrangement and that positive spin is induced in the planar zigzag conformation (Table III), in accord with the experimental trend. To further substantiate the direct "through-space" spin transmission for the planar zigzag model, we then neglected the Fock's matrix elements between the C(1) carbon (the radical center) and C(3) in the INDO-UHF MO calculations.²⁰ This procedure, which does not take into account C(1)-C(3) "through-space" interaction, yields alternating signs of the calculated spin densities on the carbon 2s orbitals along the σ bonds, and results in the negative spin density on the C(4) carbon (see Table III). The signs of calculated spin densities in the carbon with and without through-space interaction are schematically depicted below. Inclusion of the C(1)-C(3) interaction is therefore responsible for positive spin densities on C(4). It is also to be noted that the C(1)-C(3) interaction causes a small decrease in the positive

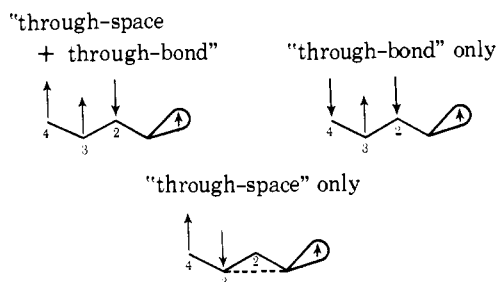
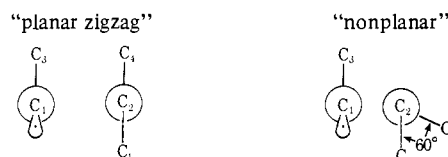


Table III. The Calculated Spin Densities with and without "Through-Space" Interaction

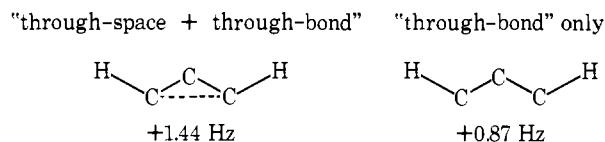
n -Butyl σ -radical	Position	"Through-space" + "through-bond" C_{2s}^a	"Through-bond" C_{2s}^b
(planar zigzag) ^d	C(2)	-0.0085 (-1.00) ^c	-0.0085 (-1.00) ^c
	C(3)	+0.0147 (+1.25)	+0.0160 (+1.89)
	C(4)	+0.0009 (+0.11)	-0.0000 (-0.00)
(nonplanar) ^d	C(2)	-0.0084 (-1.00)	-0.0083 (-1.00)
	C(3)	+0.0145 (+1.72)	+0.0156 (+1.88)
	C(4)	-0.0002 (-0.03)	-0.0004 (-0.05)

^a Spin density on the 2s AO of the carbon atom obtained by the usual calculation. ^b Obtained by the modified calculation. ^c Relative values are given in parentheses. ^d Tetrahedral configuration at each carbon. The conformation is as shown below.



spin density on C(3) (Table III), presumably due to contribution of negative spin density induced on C(3). These through-space effects are explainable in terms of spin transmission by the *through-space spin polarization mechanism* in the mode of $C(1)(\uparrow)\cdots C(3)(\downarrow)-C(4)(\uparrow)$. Contrary to this, neglect of C(1)-C(3) direct interaction hardly affects the mode of electron spin transmission for the nonplanar model (see Table II). We conclude, therefore, from these results that in the planar conformation the "through-space" spin transmission contributes substantially to the stereospecific spin distribution.²¹

This specific feature of electron spin distribution in the planar zigzag arrangement may also be important in the interpretation of the stereospecificity of the long-range H-H spin coupling constant across four σ bonds ($^4J_{H-H}$) in the "W" letter arrangement. The value of $^4J_{H-H}$ in this skeleton has been reported to be positive and amounts to 1-2 Hz.^{19,22,23} This large positive value of the long-range H-H coupling constant is explainable by the above stereospecific through-space spin transmission in the following way. We calculated the long-range H-H coupling constant $^4J_{H-H}$ using Pople's finite perturbation theory,²⁴ in which J_{H-H} is obtained from the spin density induced on H_i when spin density is finitely placed at H_j by introducing slightly different value of Fock matrices for α and β spin orbitals. Here we employed two different ways of INDO-UHF finite perturbational calculations of $^4J_{H-H}$ with and without C(1)-C(3) "through-space" interaction in a similar way stated above. This through-space interaction corresponds to well-documented "rear side lobe interaction" in the preferable H-H coupling path of "W" letter arrangement. The calculated results are shown below. This may allow us to see that inclusion of the C(1) \cdots C(3) direct interaction (F_{13}) enhances substantially the positive value of $^4J_{H-H}$ and



that "through-space" interaction plays also an important role in the long range H-H coupling associated with the planar zigzag arrangement.²³ The positive value of meta H-H coupling in benzene may be also interpreted along this line.

Summarizing the above results and discussion, we can conclude that $Ni(AA)_2$ -induced NMR contact shifts could serve as a quite sensitive probe for elucidation of modes and

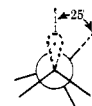
mechanisms of intramolecular electron spin transmission through the σ -bonded skeleton.

Acknowledgment. We thank Dr. W. N. Speckamp, Professors P. G. Gassman, and C. F. Hammer for the gift of the sample. We are grateful to Professor T. Yonezawa for encouragement of this work. We wish to express our appreciation to the Data Processing Center of Kyoto University for the use of the FACOM 230-60 computer. This work is supported in part by a grant from Kawakami Memorial Foundation.

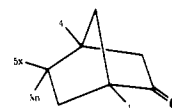
References and Notes

- (1) A part of our systematic investigation on NMR contact shift studies for the σ -bonded molecules.
- (2) (a) T. Yonezawa, I. Morishima, and Y. Ohmori, *J. Am. Chem. Soc.*, **92**, 1267 (1970); (b) I. Morishima, T. Yonezawa, and K. Goto, *ibid.*, **92**, 6651 (1970); (c) I. Morishima, K. Okada, M. Ohashi, and T. Yonezawa, *J. Chem. Soc., Chem. Commun.*, 33 (1971); (d) I. Morishima, K. Okada, T. Yonezawa, and K. Goto, *J. Am. Chem. Soc.*, **93**, 3922 (1971); (e) I. Morishima, K. Okada, and T. Yonezawa, *ibid.*, **94**, 1425 (1972); (f) I. Morishima and K. Yoshikawa, *ibid.*, **97**, 2950 (1975).
- (3) The observed shifts in Ni(AA)₂ complexes are caused only by contact interaction; ref 2 and 17, and references cited therein.
- (4) The Ni(AA)₂-induced ¹H and ¹³C contact shift study appears to be relevant for elucidation of the mode of intramolecular electron spin distribution because the contact shift is quite sensitive to both quantity and sign of the induced spin density. It appears to excel the ESR study, especially in its availability of the ¹³C contact shift which is related to spin density on the carbon skeleton. In this sense Ni(AA)₂-induced contact shift is referred to as a "spin probe" for elucidation of the electronic and geometrical structure of the σ -bonded molecules.
- (5) G. M. Zhidomirov and N. D. Chuvylkin, *Teor. Eksp. Khim.*, **6**, 254 (1970); G. M. Zhidomirov, P. V. Schastnev, and N. D. Chuvylkin, *Zh. Strukt. Khim.*, **11**, 502 (1970); (c) N. D. Chuvylkin, R. Z. Sagdeev, G. M. Zhidomirov, and Yu. N. Molin, *Teor. Eksp. Khim.*, **7**, 612 (1971); R. Z. Sagdeev and Yu. N. Molin, *Chem. Phys. Lett.*, **5**, 471 (1970).
- (6) M. S. Sun, F. Grein, and D. G. Brewer, *Can. J. Chem.*, **50**, 2626 (1972).
- (7) W. T. Dixon, *Mol. Phys.*, **11**, 601 (1966).
- (8) M. Barfield and B. Chakrabarti, *Chem. Rev.*, **69**, 757 (1969).
- (9) J. W. McIver, Jr., and G. E. Maciel, *J. Am. Chem. Soc.*, **93**, 4641 (1971).
- (10) I. Morishima and T. Yonezawa, *J. Chem. Phys.*, **54**, 3238 (1971).
- (11) Z. Luz, *J. Chem. Phys.*, **48**, 4186 (1968).
- (12) H. T. Clarke, H. B. Gillespie, and S. Z. Weisshaus, *J. Am. Chem. Soc.*, **55**, 4571 (1933).
- (13) I. Morishima, K. Yoshikawa, K. Okada, T. Yonezawa, and K. Goto, *J. Am. Chem. Soc.*, **95**, 165 (1973).

- (14) In the MO calculation, all the bond angles were tetrahedral. The dihedral angle in the model of 1-bicyclo[3.2.1]octyl radical was taken to be 25°, which is assumed from the molecular model of 10.



- (15) Similar MO calculation for 1-propyl σ radical have been reported; G. R. Underwood, V. L. Vogel, and J.-A. Iorlo, *Mol. Phys.*, **25**, 1093 (1973).
- (16) M. Karplus, *J. Chem. Phys.*, **30**, 11 (1959).
- (17) (a) T. Yonezawa, H. Nakatsuji, T. Kawamura, and H. Kato, *Chem. Phys. Lett.*, **2**, 454 (1968); *J. Chem. Phys.*, **51**, 669 (1969); *Bull. Chem. Soc. Jpn.*, **42**, 2437 (1969); (b) H. Nakatsuji, H. Kato, and T. Yonezawa, *J. Chem. Phys.*, **51**, 3175 (1969).
- (18) D. Doddrell and J. D. Roberts, *J. Am. Chem. Soc.*, **92**, 6839 (1970).
- (19) Similar experimental trend of H-H coupling constants in norcamphor has been reported. Coupling constants are $J_{1,4} = +1.17$, $J_{1,5x} = +0.15$, $J_{1,5n} = -0.30$. It is noticeable that $J_{1,4}$ and $J_{1,5x}$ are positive, which is in contrast with the negative value of $J_{1,5n}$; J. L. Marshall and S. R. Walter, *J. Am. Chem. Soc.*, **96**, 6358 (1974).



- (20) A referee pointed out that in a SCF theory neglecting the Fock matrix elements would modify the "through-bond" contribution. In order to avoid such an influence, the neglect has been carried out after the conversion of the normal SCF calculations. Therefore, the modification of the "through-bond" contribution is considered to be minimum.
- (21) Recently Kawamura et al. suggested, based on the ESR study, that the odd electron is delocalized onto the bridgehead atom through a "through-space" mechanism in the case of the 1-norbornyl radical; T. Kawamura, M. Matsumaga, and T. Yonezawa, *J. Am. Chem. Soc.*, **97**, 3235 (1975).
- (22) See, for example, L. M. Jackman and S. Sternhell, "Application of Nuclear Magnetic Resonance Spectroscopy in Organic Chemistry", 2d ed, Pergamon Press, Oxford, 1969, Chapter 4.
- (23) From the MO calculations, Barfield et al. concluded that the substantial positive value for propanoic coupling in the "W" conformation arises from a direct mechanism which overcomes a negative indirect mechanism; M. Barfield, A. M. Dean, C. J. Fallick, R. J. Spear, S. Sternhell, and P. W. Westerman, *J. Am. Chem. Soc.*, **97**, 1482 (1975).
- (24) J. A. Pople, J. W. McIver, Jr., and N. S. Ostlund, *J. Chem. Phys.*, **49**, 2960, 2965 (1968).

Stable Hydrogen-Bonded Adducts of Unstable Polyhalogenated *gem*-Diols

E. M. Schulman,* O. D. Bonner, D. R. Schulman, and F. M. Laskovics

Contribution from the Department of Chemistry, University of South Carolina, Columbia, South Carolina 29208. Received August 11, 1975

Abstract: Stable adducts involving the *gem*-diols of hydrated hexachloroacetone, pentachloroacetone, 1,3-difluorotetrachloroacetone, and chloral have been formed with several classes of organic acceptors. Although some of the hydrates themselves are stable, e.g., chloral hydrate, others are not, e.g., hexachloroacetone hydrate; however, all of the adducts formed with organic acceptors are quite stable, several being crystalline solids. The stability exhibited by these adducts is believed to originate from the formation of two strong hydrogen bonds. Spectral evidence supporting the formation of a *gem*-diol from the halogenated ketones and its hydrogen bonding to an organic acceptor comes from the disappearance of water absorption in the near ir when a halogenated ketone is added to a "wet" organic acceptor, the absence of the ir carbonyl absorption of the halogenated ketone in the adducts, and the large shifts observed in the ir and Raman absorptions of oxygen functionalities of the organic acceptors upon adduct formation. Possible adduct structures, inferred from the spectral data, are also presented. The Raman spectrum of hexachloroacetone hydrate, an unstable crystalline material previously thought to be a monohydrate, has been obtained and has been shown to be a tetrahydrate by quantitative gas chromatography.

Highly halogenated ketones and aldehydes are expected to form stable hydrates due to the electronegativity of the groups attached to the carbonyl carbon. Thus, stable hydrates are formed from halogenated ethanals and highly fluorinated acetones.¹ These *gem*-diols have been very useful as solvents

for polymers and biological membranes² due to their ability to form strong hydrogen bonds. Although halogenated ethanal hydrates and hydrates of fluoro ketones are stable *gem*-diols, forming spontaneously when the carbonyl compounds are exposed to moist air, hexachloroacetone can be shaken with